PHYSICAL REVIEW B **96**, 165123 (2017)

Topological Dirac line nodes and superconductivity coexist in SnSe at high pressure

Xuliang Chen,[1] Pengchao Lu,[2] Xuefei Wang,[1] Yonghui Zhou,[1] Chao An,[1] Ying Zhou,[1] Cong Xian,[1] Hao Gao,[2]
Zhaopeng Guo,[2] Changyong Park,[3] Binyang Hou,[3] Kunling Peng,[4] Xiaoyuan Zhou,[4] Jian Sun,[2,5,*] Yimin Xiong,[1,5,†]
Zhaorong Yang,[1,5,6,‡] Dingyu Xing,[2,5] and Yuheng Zhang[1,5]

[1]*Anhui Province Key Laboratory of Condensed Matter Physics at Extreme Conditions, High Magnetic Field Laboratory, Chinese Academy of Sciences, Hefei 230031, China*
[2]*National Laboratory of Solid State Microstructures, School of Physics, Nanjing University, Nanjing 210093, China*
[3]*HPCAT, Geophysical Laboratory, Carnegie Institution of Washington, Argonne, Illinois 60439, USA*
[4]*College of Physics, Chongqing University, Chongqing 401331, China*
[5]*Collaborative Innovation Center of Advanced Microstructures, Nanjing 210093, China*
[6]*Key Laboratory of Materials Physics, Institute of Solid State Physics, Chinese Academy of Sciences, Hefei 230031, China*

(Received 17 March 2017; revised manuscript received 23 June 2017; published 12 October 2017)

We report on the discovery of a pressure-induced topological and superconducting phase of SnSe, a material which attracts much attention recently due to its superior thermoelectric properties. *In situ* high-pressure electrical transport and synchrotron x-ray diffraction measurements show that the superconductivity emerges along with the formation of a CsCl-type structural phase of SnSe above around 27 GPa, with a maximum critical temperature of 3.2 K at 39 GPa. Based on *ab initio* calculations, this CsCl-type SnSe is predicted to be a Dirac line-node (DLN) semimetal in the absence of spin-orbit coupling, whose DLN states are protected by the coexistence of time-reversal and inversion symmetries. These results make CsCl-type SnSe an interesting model platform with simple crystal symmetry to study the interplay of topological physics and superconductivity.

DOI: 10.1103/PhysRevB.96.165123

The search for topological superconductivity and exotic fermions such as Majorana quasiparticles has been a rapidly growing research field in condensed matter physics for both fundamental interests and potential applications in fault-tolerant topological quantum computation [1,2]. Several methods have been proposed and applied to realize topological superconductivity, such as using the proximity effect at the interface between a topological insulator and superconductor [3,4] or nanowire [5,6], doping a topological insulator [7,8], as well as compressing a topological insulator or a topological semimetal [9–17]. Among the above methods, application of external pressure is considered as a clean and effective way to tune lattice as well as electronic states, especially for the study of topological materials and their possible bulk superconductivity [10–17]. However, the coexistence of superconductivity and topological properties under pressure is not obvious, for instance, the high pressure phase of TaAs is a new Weyl semimetal but it is not superconducting [18], and the superconductivity emerges in WTe_2 under pressure while its Weyl nodes disappear [19].

Like the topological insulators Bi_2Se_3 and Bi_2Te_3 [20,21], SnSe is known as an excellent thermoelectric material, with a record figure of merit of 2.6 ± 0.3 at 923 K along the *b* axis [22,23]. Under ambient conditions, SnSe is an ordinary semiconductor and has a layered orthorhombic (*Pnma*, No. 62) GeS-type crystal structure [24]. Interestingly, SnSe with cubic NaCl-type structure was theoretically proposed to be a native topological crystalline insulator [25] with surface states protected by mirror symmetry [25–29]. By means of strain generated from lattice mismatch between SnSe and the substrate in epitaxial films, metastable NaCl-type SnSe was realized, displaying Dirac surface states on the basis of angle-resolved photoemission spectroscopy [30]. Under applied pressures to around 30 GPa, SnSe was reported to undergo an orthorhombic ($Pnma$) to orthorhombic ($Cmcm$ or $Bbmm$, No. 63) structural transition at ~10 GPa [31–36]. Being accompanied by the structural transition, a semiconductor to semimetal transition with abnormal enhancements in carrier concentration and mobility was observed [24]. Timofeev *et al.* [37] claimed the discovery of superconductivity in SnSe with T_C around 4.5 K at 58 GPa, however, without giving any experimental curve. Obviously, the detailed properties of SnSe at pressures higher than 30 GPa remain far from being well explored.

In this paper, we present a pressure-induced superconducting transition and a topological phase transition in SnSe. By *in situ* high pressure synchrotron x-ray diffraction and electrical transport measurements, a new phase of SnSe in CsCl-type structure is observed above around 27 GPa and this new phase is found to be superconducting. Theoretical calculations reveal that this CsCl-type SnSe has a unique electronic feature with Dirac line nodes and topological surface states, which might have contributions to the observed superconductivity when the system is doped. The simultaneous presence of nontrivial topology and superconductivity makes SnSe a promising material to study the correlations between them.

Experimental details and theoretical calculations are presented in the Supplemental Material [38]. *In situ* high-pressure angular dispersive synchrotron x-ray diffraction (XRD) experiments were performed with the SnSe sample up to 50.1 GPa at room temperature ($\lambda = 0.4246$ Å). The experimental results are presented in Fig. 1(a) (see also Fig. S1 for more details). Standard Rietveld refinements were performed using the GSAS program [39]. Starting at 1.3 GPa, the pattern can be indexed solely by the GeS-type orthorhombic structure with space

---

[*] jiansun@nju.edu.cn
[†] yxiong@hmfl.ac.cn
[‡] zryang@issp.ac.cn

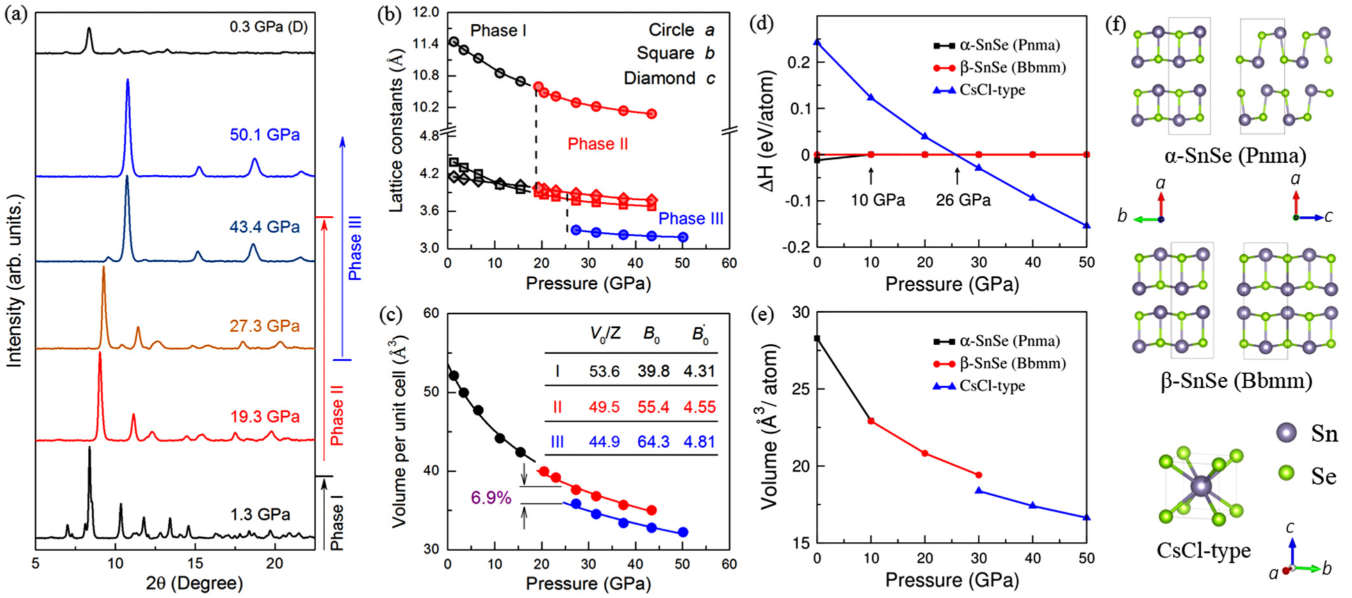

FIG. 1. (a) *In situ* high-pressure angular dispersive synchrotron XRD of SnSe at room temperature ($\lambda = 0.4246$ Å). (b) Lattice parameters as a function of pressure. (c) The compression data was fitted by the third-order Birch-Murnaghan equation of state (solid lines). (d) Calculated enthalpy relative to that of the β-SnSe ($Bbmm$) at pressure up to 50 GPa. (e) Unit cell volume versus pressure. (f) Crystal structures of α-SnSe ($Pnma$), β-SnSe and CsCl-type SnSe ($Pm\bar{3}m$). With increasing pressure, there are two transitions from α-SnSe to β-SnSe at around 10 GPa and further to CsCl-type SnSe at about 26 GPa.

group $Pnma$ (No. 62), labeled as Phase I (black), which is the same as that of SnSe at ambient conditions [40]. Above 15.5 GPa, the lattice structure (Phase II, red) can be described by space group $Bbmm$ (No. 63), which is a nonstandard setting of space group $Cmcm$ (No. 63). Such structural transition of $Pnma \rightarrow Bbmm$ (or $Cmcm$) under pressure was also reported by previous work [31–33]. In the pressure range of 27.3–43.4 GPa, the XRD pattern is a superposition of Phase II and Phase III. At 50.1 GPa (Phase III, blue), the XRD peaks can be indexed by the CsCl-type with space group $Pm\bar{3}m$ (No. 221). When decompressing back to 0.3 GPa (denoted by D), the XRD pattern came back to the starting structure, manifesting that the pressure-driven structural transition is reversible. Figures 1(b) and 1(c) show the variations in lattice parameters as a function of pressure and the isothermal equations of state (EoS), which evidences that the low- and high-pressure structural transitions are of second and first order, respectively. We also calculated the high-pressure structures of SnSe and the EoS by using the *ab initio* random structure searching method, which agrees excellently with our experimental results [see Figs. 1(d) and 1(f)]. More discussion on the pressure-driven structural transitions, selected XRD refinements, and the corresponding results can be found in Fig. S2 and Table S1 in the Supplemental Material [38].

Electronic structures of CsCl-type SnSe are further calculated, shown in Fig. 2. Analysis of electronic structures implies that the CsCl-type SnSe should be a topological metal with Dirac line nodes (DLN) if spin-orbit coupling (SOC) is ignored. There are two band crossings along the M-X and X-R lines [Fig. 2(a)], indicating a DLN ring encircling the X point on the R-X-M plane. The point group along the M-X line is C_{2v}, which allows two different irreducible representations (Γ_1 and Γ_4) and protects these two bands from hybridization. A similar situation applies for the X-R line. As there is only one irreducible representation Γ_5 belonging to the C_{2v} double group, it opens a gap when SOC is included, as shown in Fig. 2(b). Due to the coexistence of inversion and time-reversal symmetries as well as a continuous band gap, one can obtain the Z_2 topological invariant by calculating the parity products of occupied states at eight time-reversal-invariant momenta (TRIM) points [41–44]. For both the $Pnma$ and $Bbmm$ phases, a trivial Z_2 of (0;000) is given (see Table S2); however, for the CsCl-type SnSe, the calculation gives the Z_2 topological invariant ($\nu_0;\nu_1\nu_2\nu_3$) as (1;111). We find that the parity at X is opposite from those at all other TRIM, as shown in Table I, which is attributed to the inversion of the conduction Γ_2^- and valence Γ_1^+ states at X. The change of the Z_2 invariant from the $Bbmm$ to CsCl-type phases indicates a topological phase transition, accompanied by the structural transition.

In general, DLNs suggest existence of topologically nontrivial surface states, called "flat band," which is considered as a way to induce high-temperature superconductivity [45–47]. We calculated the surface band structures of the semi-infinite (100) surface with two different terminations, say Sn and Se shown in Figs. 2(c) and 2(d), respectively. It can be seen that there are several nontrivial surface bands connecting with Dirac nodes in the absence of SOC. In contrast to trivial surface states from the dangling bonds, these nontrivial surface states emerge as a characterization of the bulk electronic structure and are protected by time-reversal symmetry [48]. Due to the existence of a nonzero Z_2, they are stable with respect to SOC, though it opens a gap of around 0.2 eV for the bulk states. These nontrivial states show local flatness in some places, for example, the surface states along $\bar{\Gamma}$-$\bar{X}$ with Se termination seem nearly flat. Although the CsCl-structured SnSe is a metal due to the fact that there are several bands crossing the Fermi

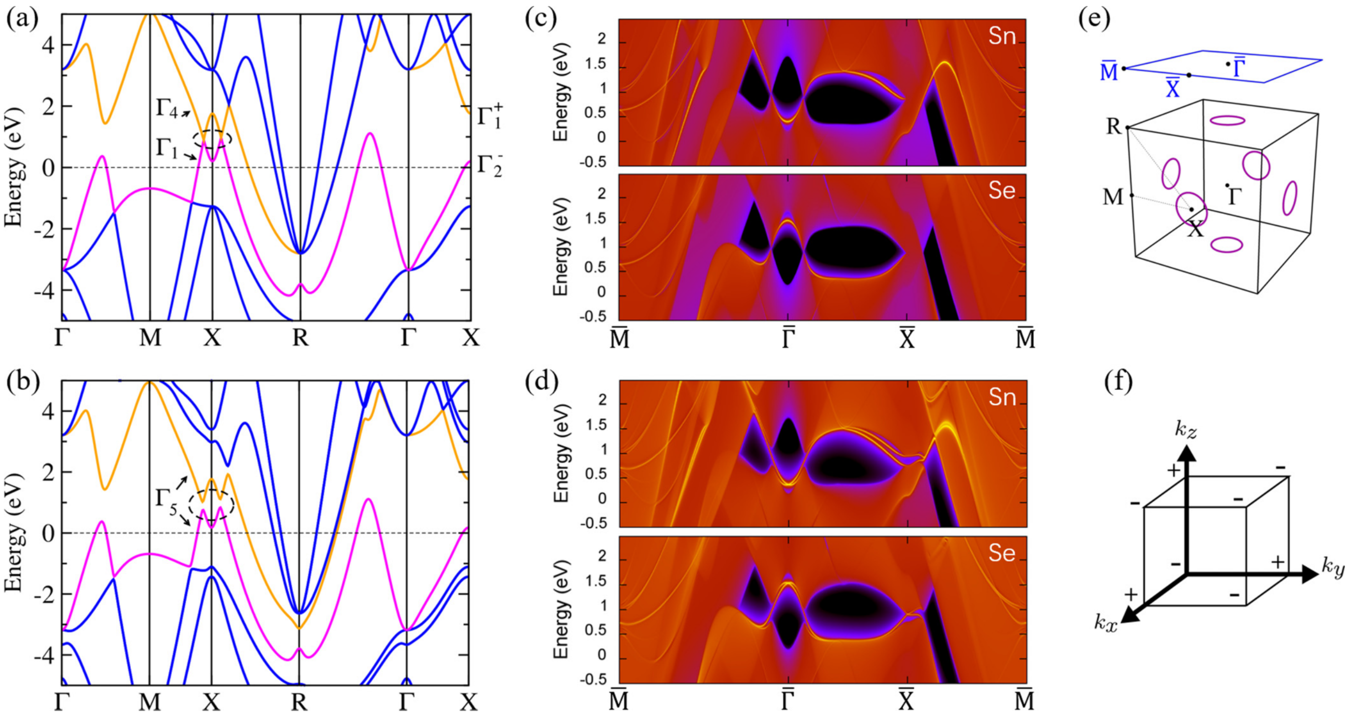

FIG. 2. Calculated electronic structures of bulk CsCl-type SnSe at 40 GPa (a) without SOC and (b) with SOC. Surface band structures (c) without SOC and (d) with SOC for the semi-infinite (100) surface, with Sn (upper panel) and Se (lower panel) terminations, respectively. (e) Bulk and projected (001) surface Brillouin zone (BZ). (f) Parity products of occupied states at the eight TRIM points in the first octant of the BZ.

level, however, from the topological point of view, there exists a continuous "band gap" and nontrivial surface states, thus this phase can be considered as a strong topological insulatorlike material in the presence of SOC.

To investigate the experimental manifestations of the nontrivial band topology in electronic properties, we carried out electrical transport measurements on single crystal SnSe up to 55.0 GPa. Figures 3(a)–3(d) shows the temperature dependence of the dc electrical resistance of SnSe in the temperature range of 1.8–300 K. At 0.4 GPa, a semiconducting behavior ($dR/dT < 0$) is observed in the whole temperature range as that of semiconducting SnSe at ambient pressure [24,49]. With increasing pressure, the whole resistance decreases rapidly implying a remarkable reduction in energy gap of the material with pressure (see Fig. S4). At 12.0 GPa, a typical metallic character over the entire temperature range is observed. At the same time, the resistance at 2 K drops about six orders in magnitude with respect to that of 0.4 GPa. These observations evidence a transition of SnSe from semiconductor to metal under pressure. Here the critical pressure (12.0 GPa) of metallization for SnSe is in excellent accordance with the one (12.6 GPa) obtained from previous resistance experiments although the latter was performed in a temperature range of 80–270 K [24]. When the pressure goes up to 17.3 GPa, however, the resistance reveals an abnormal overall rise in addition to the metallic behavior, as indicated by the dashed line in Fig. 3(b). This can be ascribed to the structural transition from Phase I to Phase II.

TABLE I. Parity product of occupied states at the TRIM points, indicating the Z_2 indices as (1;111).

TRIM	Γ	R	M (×3)	X (×3)
Parity product	−	−	−	+

Upon further compression, the resistance becomes increasingly metallic. The most striking finding is that at 27.2 GPa a drop of resistance is initially observed below about 2.5 K as presented in Fig. 3(c) and in Fig. 3(d), an enlarged view of the low temperature region of resistance. This sharp drop should be a signal of a superconducting transition as zero resistance is observed at 2 K at 34.3 GPa. The critical temperature T_C is defined as the onset of the superconducting phase transition. Further increasing pressure, it first increases slightly, reaches a maximum of about 3.2 K at 39.0 GPa, and then decreases gradually to 2.5 K at 55.0 GPa.

To further confirm that the drop in resistance belongs to a superconducting transition, we measured the low temperature resistance at 39.0 GPa under applied magnetic fields parallel to the [100] direction, as displayed in Fig. 3(e). With increasing field, T_C decreases gradually and the resistance drop was almost smeared out at 0.5 T, which confirms that the drop of resistance is the superconducting transition. We have plotted the upper critical field H_{C2} as a function of temperature in Fig. 3(f). Here $H_{C2}(T)$ is defined from the resistance criterion of $R_{\text{cri}} = 90\% R_n$ (R_n is the normal state resistance near T_C). One can see that H_{C2} follows a linear dependence in temperature (red dashed line). By extrapolating it to zero temperature, $H_{C2}(0)$ is estimated to be 1.12 T. Here, the Pauli

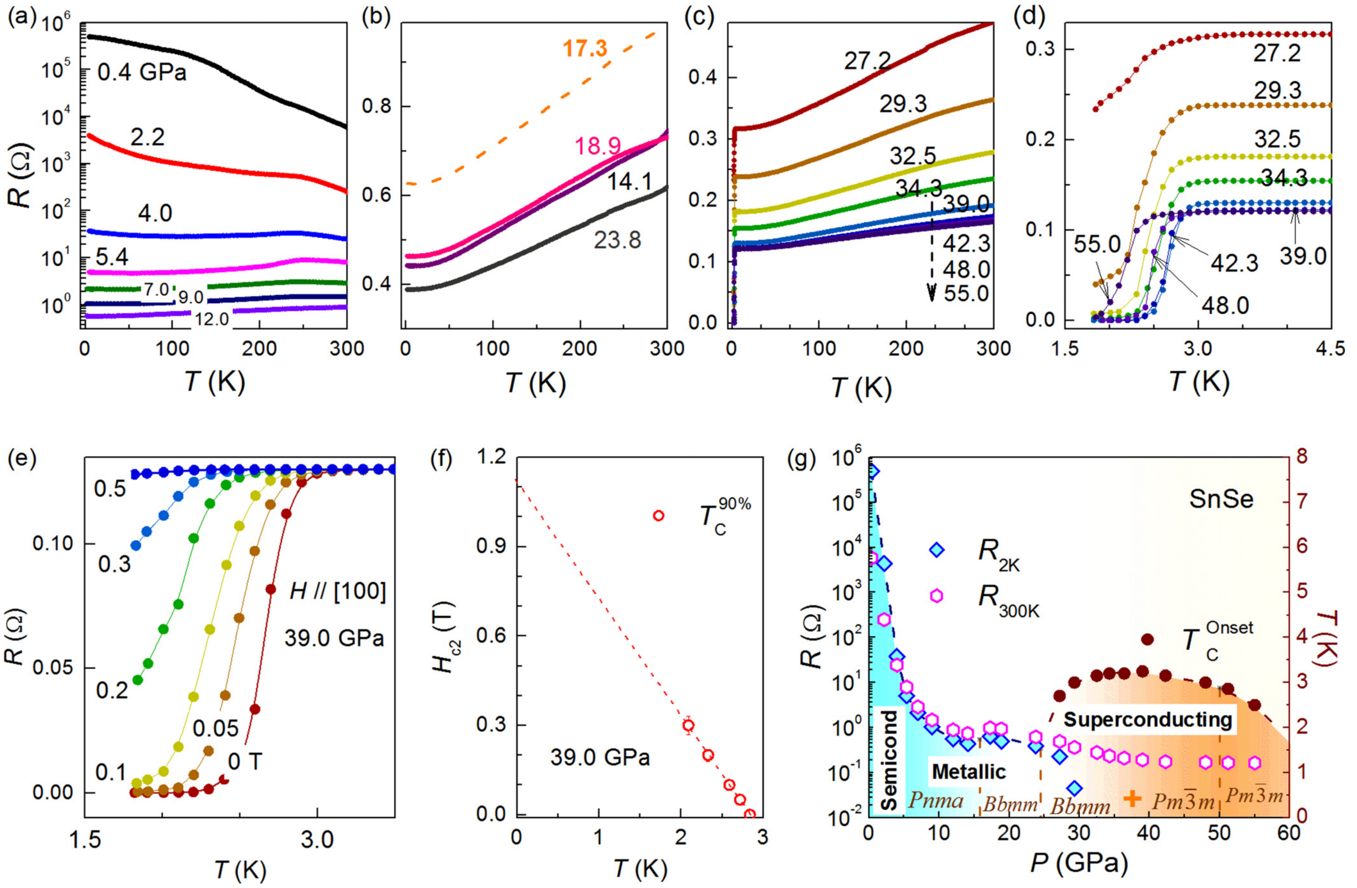

FIG. 3. (a)–(c) Temperature-dependent resistance for SnSe single crystal. (d) An enlarged view of the low temperature resistance above 27.2 GPa, showing the superconducting transition. (e) The superconducting transition of the SnSe single crystal in magnetic fields up to 0.5 T with $H//[100]$. (f) Temperature dependence of the upper critical field H_{C2}. T_C is determined as the 90% drop of the normal state resistance. The dashed line is a linear fit to the data and $H_{C2}(0)$ is estimated to be 1.12 T. (g) Temperature versus pressure phase diagram. The left axis stands for the resistance R at 2 and 300 K and the right axis corresponds to temperature T.

paramagnetic effect does not apply since the Pauli limiting field is about 5.4 T ($1.84\times T_C$), suggestive of an absence of Pauli pair breaking.

As outlined in Fig. 3(g), the present XRD results evidence a set of structural transitions. Correspondingly, the nearest coordination numbers of Sn increase sequentially from three to five, and five to eight [Fig. 1(f)]. Superconductivity is only observed being accompanied by the appearance of the high pressure CsCl-type phase. In addition, owing to the coexistence of the nonsuperconducting *Bbmm* and superconducting $Pm\bar{3}m$ structures, superconductivity first shows up at 27.2 GPa and zero resistance is observed above 34.3 GPa [Fig. 3(d)].

Recently, a large amount of effort has been devoted to exploring possible topological superconductivity from topological materials by external pressure, such as Bi_2Se_3 [12,50], Bi_2Te_3 [10,51], $ZrTe_5$ [16], Cd_3As_2 [17], Sr doped Bi_2Se_3 [52], etc. However, one may find that the appearance of superconductivity is generally along with a structural transition, making it an open question on the topological nature of the pressure-induced superconducting states in these materials. Here, the coexistence of the nontrivial topological feature of electronic band and superconductivity should be of special interest. We tried to study the predicted nontrivial band topology via high-pressure magnetotransport experiments; see Fig. S5. Unfortunately, no evident SdH oscillations of the magnetoresistance is observed for SnSe at 1.8/5 K, up to 25 T and 57.0 GPa, which could be attributed to the sample inhomogeneity under high pressure [53], despite the predicted Dirac-like dispersion of high-pressure SnSe. Nevertheless, we noted that the magnitude of the low temperature resistance in the normal state keeps almost unchanged, i.e., showing pressure- and temperature-independent behaviors (above ~50 GPa; below ~20 K), see Fig. 3(c) and Fig. S5 in both runs. As a matter of fact, such temperature independent electronic transport behavior has also been observed in other topological materials, which was related to the topological properties [54,55].

In summary, we observed the formation of a new topological and superconducting CsCl-type phase of SnSe under high pressures based on experiments coupled with theoretical calculations. We found that this new phase appears at 27 GPa and coexists with the *Bbmm* phase in a broad pressure range, and eventually a pure CsCl-type phase establishes above 50 GPa. Our electronic transport measurements discovered a pressure-driven superconductivity rooted in this CsCl-type phase. In view of *ab initio* calculations, we predict that CsCl-type SnSe is a DLN semimetal, involving nontrivial topological surface states which are stable against SOC. Further experiments are required to confirm our theoretical prediction. Once doping is introduced in SnSe to make the DLN or nontrivial states closer to or even crossing the Fermi level, more novel phenomena may be induced by pressure. It is thus proposed that SnSe may provide a model platform with high crystal symmetry to investigate the topological characteristics of electronic structures and their correlations to superconductivity.

The authors thank Prof. X. Chen for stimulating discussions. This work is supported by the National Key Research and Development Program of China (Grants No. 2016YFA0300404, No. 2016YFA0401804, and No. 2015CB921202), and the NSFC (Grants No. 11574323, No. 11474288, No. 51472036, No. 51372112, No. 11574133, and No. U1632275), NSF Anhui Province (1708085QA19), NSF Jiangsu Province (BK20150012), the Fundamental Research Funds for the Central Universities (No. 020414380068/1-1) and Special Program for Applied Research on Super Computation of the NSFC-Guangdong Joint Fund (the 2nd phase). Part of the calculations were performed on the supercomputer at HPCC in Nanjing University and "Tianhe 2" at NSCC Guangzhou. Y.X. acknowledges the support of the Hundred Talents Program of the Chinese Academy of Science. The authors acknowledge the photoemission spectroscopy beamline (BL10B) at the NSRL for providing the beam time for the XPS experiment. The x-ray work was performed at HPCAT (Sector 16), APS of ANL. HPCAT operations are supported by DOE-NNSA under Award No. DE-NA0001974 and DOE-BES under Award No. DE-FG02-99ER45775, with partial instrumentation funding by NSF. The APS is a U.S. Department of Energy (DOE) Office of Science User Facility operated for the DOE Office of Science by ANL under Contract No. DE-AC02-06CH11357.

X. L. Chen and P. C. Lu contributed equally to this work.

---

[1] X.-L. Qi and S.-C. Zhang, Rev. Mod. Phys. **83**, 1057 (2011).

[2] M. Z. Hasan, S.-Y. Xu, and G. Bian, Phys. Scr. **T168**, 019501 (2016).

[3] L. Fu and C. L. Kane, Phys. Rev. Lett. **100**, 096407 (2008).

[4] M.-X. Wang, C. H. Liu, J.-P. Xu, F. Yang, L. Miao, M.-Y. Yao, C. L. Gao, C. Y. Shen, X. C. Ma, X. Chen, Z.-A. Xu, Y. Liu, S.-C. Zhang, D. Qian, J.-F. Jia, and Q.-K. Xue, Science **336**, 52 (2012).

[5] V. Mourik, K. Zuo, S. M. Frolov, S. R. Plissard, E. P. A. M. Bakkers, and L. P. Kouwenhoven, Science **336**, 1003 (2012).

[6] A. Das, Y. Ronen, Y. Most, Y. Oreg, M. Heiblum, and H. Shtrikman, Nat. Phys. **8**, 887 (2012).

[7] S. Sasaki, M. Kriener, K. Segawa, K. Yada, Y. Tanaka, M. Sato, and Y. Ando, Phys. Rev. Lett. **107**, 217001 (2011).

[8] L. A. Wray, S.-Y. Xu, Y. Q. Xia, Y. S. Hor, D. Qian, A. V. Fedorov, H. Lin, A. Bansil, R. J. Cava, and M. Z. Hasan, Nat. Phys. **6**, 855 (2010).

[9] T. V. Bay, T. Naka, Y. K. Huang, H. Luigjes, M. S. Golden, and A. de Visser, Phys. Rev. Lett. **108**, 057001 (2012).

[10] J. L. Zhang, S. J. Zhang, H. M. Weng, W. Zhang, L. X. Yang, Q. Q. Liu, S. M. Feng, X. C. Wang, R. C. Yu, L. Z. Cao, L. Wang, W. G. Yang, H. Z. Liu, W. Y. Zhao, S. C. Zhang, X. Dai, Z. Fang, and C. Q. Jin, Proc. Natl. Acad. Sci. USA **108**, 24 (2011).

[11] C. Zhang, L. L. Sun, Z. Y. Chen, X. J. Zhou, Q. Wu, W. Yi, J. Guo, X. L. Dong, and Z. X. Zhao, Phys. Rev. B **83**, 140504(R) (2011).

[12] K. Kirshenbaum, P. S. Syers, A. P. Hope, N. P. Butch, J. R. Jeffries, S. T. Weir, J. J. Hamlin, M. B. Maple, Y. K. Vohra, and J. Paglione, Phys. Rev. Lett. **111**, 087001 (2013).

[13] D. F. Kang, Y. Z. Zhou, W. Yi, C. L. Yang, J. Guo, Y. G. Shi, S. Zhang, Z. Wang, C. Zhang, S. Jiang, A. G. Li, K. Yang, Q. Wu, G. M. Zhang, L. L. Sun, and Z. X. Zhao, Nat. Commun. **6**, 7804 (2015).

[14] X.-C. Pan, X. L. Chen, H. M. Liu, Y. Q. Feng, Z. X. Wei, Y. H. Zhou, Z. C. Chi, L. Pi, F. Yen, F. Q. Song, X. G. Wan, Z. R. Yang, B. G. Wang, G. H. Wang, and Y. H. Zhang, Nat. Commun. **6**, 7805 (2015).

[15] Y. P. Qi, P. G. Naumov, M. N. Ali, C. R. Rajamathi, W. Schnelle, O. Barkalov, M. Hanfland, S.-C. Wu, C. Shekhar, Y. Sun, V. Süß, M. Schmidt, U. Schwarz, E. Pippel, P. Werner, R. Hillebrand, T. Förster, E. Kampert, S. Parkin, R. J. Cava, C. Felser, B. H. Yan, and S. A. Medvedev, Nat. Commun. **7**, 11038 (2016).

[16] Y. H. Zhou, J. F. Wu, W. Ning, N. N. Li, Y. P. Du, X. L. Chen, R. R. Zhang, Z. H. Chi, X. F. Wang, X. D. Zhu, P. C. Lu, C. Ji, X. G. Wan, Z. R. Yang, J. Sun, W. G. Yang, M. L. Tian, Y. H. Zhang, and H.-K. Mao, Proc. Natl. Acad. Sci. USA **113**, 2904 (2016).

[17] L. P. He, Y. T. Jia, S. J. Zhang, X. C. Hong, C. Q. Jin, and S. Y. Li, npj Quantum Mater. **1**, 16014 (2016).

[18] Y. H. Zhou, P. C. Lu, Y. P. Du, X. D. Zhu, G. H. Zhang, R. R. Zhang, D. X. Shao, X. L. Chen, X. F. Wang, M. L. Tian, J. Sun, X. G. Wan, Z. R. Yang, W. G. Yang, Y. H. Zhang, and D. Y. Xing, Phys. Rev. Lett. **117**, 146402 (2016).

[19] P. C. Lu, J.-S. Kim, J. Yang, H. Gao, J. F. Wu, D. X. Shao, B. Li, D. W. Zhou, J. Sun, D. J. Akinwande, D. Y. Xing, and J.-F. Lin, Phys. Rev. B **94**, 224512 (2016).

[20] P. Ghaemi, R. S. K. Mong, and J. E. Moore, Phys. Rev. Lett. **105**, 166603 (2010).

[21] N. F. Hinsche, B. Y. Yavorsky, I. Mertig, and P. Zahn, Phys. Rev. B **84**, 165214 (2011).

[22] L.-D. Zhao, S.-H. Lo, Y. S. Zhang, H. Sun, G. J. Tan, C. Uher, C. Wolverton, V. P. Dravid, and M. G. Kanatzidis, Nature (London) **508**, 373 (2014).

[23] L.-D. Zhao, G. J. Tan, S. Q. Hao, J. Q. He, Y. L. Pei, H. Chi, H. Wang, S. K. Gong, H. B. Xu, V. P. Dravid, C. Uher, G. J. Snyder, C. Wolverton, and M. G. Kanatzidis, Science **351**, 141 (2016).

[24] J. J. Yan, F. Ke, C. L. Liu, L. Wang, Q. L. Wang, J. K. Zhang, G. H. Li, Y. H. Han, Y. Z. Ma, and C. X. Gao, Phys. Chem. Chem. Phys. **18**, 5012 (2016).

[25] Y. Sun, Z. C. Zhong, T. Shirakawa, C. Franchini, D. Z. Li, Y. Y. Li, S. Yunoki, and X.-Q. Chen, Phys. Rev. B **88**, 235122 (2013).

[26] M. Neupane, S.-Y. Xu, R. Sankar, Q. Gibson, Y. J. Wang, I. Belopolski, N. Alidoust, G. Bian, P. P. Shibayev, D. S. Sanchez, Y. Ohtsubo, A. Taleb-Ibrahimi, S. Basak, W.-F. Tsai, H. Lin, T. Durakiewicz, R. J. Cava, A. Bansil, F. C. Chou, and M. Z. Hasan, Phys. Rev. B **92**, 075131 (2015).

[27] L. Fu, Phys. Rev. Lett. **106**, 106802 (2011).

[28] Y. Ando and L. Fu, Annu. Rev. Condens. Matter Phys. **6**, 361 (2015).
[29] T. H. Hsieh, H. Lin, J. W. Liu, W. H. Duan, A. Bansil, and L. Fu, Nat. Commun. **3**, 982 (2012).
[30] Z. Y. Wang, J. F. Wang, Y. Y. Zang, Q. H. Zhang, J.-A. Shi, T. Jiang, Y. Gong, C.-L. Song, S.-H. Ji, L.-L. Wang, L. Gu, K. He, W. H. Duan, X. C. Ma, X. Chen, and Q.-K. Xue, Adv. Mater. **27**, 4150 (2015).
[31] T. Chattopadhyay, A. Werner, H. G. von Schnering, and J. Pannetier, Rev. Phys. Appl. (Paris) **19**, 807 (1984).
[32] I. Loa, R. J. Husband, R. A. Downie, S. R. Popuri, and J.-W. G. Bos, J. Phys.: Condens. Matter **27**, 072202 (2015).
[33] J. Zhang, H. Y. Zhu, X. X. Wu, H. Cui, D. M. Li, J. R. Jiang, C. X. Gao, Q. S. Wang, and Q. L. Cui, Nanoscale **7**, 10807 (2015).
[34] S. M. de Souza, H. O. da Frota, D. M. Trichês, A. Ghosh, P. Chaudhuri, M. S. dos Santos Gusmao, A. F. F. de Figueiredo Pereira, M. C. Siqueira, K. D. Machado, and J. C. de Lima, J. Appl. Cryst. **49**, 213 (2016).
[35] S. Alptekin, J. Mol. Model **17**, 2989 (2011).
[36] L. Makinistian and E. A. Albanesi, Comput. Mater. Sci. **50**, 2872 (2011).
[37] Yu. A. Timofeev, B. V. Vinogradov, and V. B. Begoulev, Phys. Solid State **39**, 207 (1997).
[38] See Supplemental Material at http://link.aps.org/supplemental/10.1103/PhysRevB.96.165123 for the band calculation, experimental details, and the supporting results, which includes Refs. [56–67].
[39] R. B. von Dreele and A. C. Larson, *Regents of the University of California* (Los Alamos National Laboratory, Los Alamos, 2001); B. H. Toby, J. Appl. Cryst. **34**, 210 (2001).
[40] T. Chattopadhyay, J. Pannetier, and H. G. von Schnering, J. Phys. Chem. Solids **47**, 879 (1986).
[41] L. Fu, C. L. Kane, and E. J. Mele, Phys. Rev. Lett. **98**, 106803 (2007).
[42] A. P. Schnyder, S. Ryu, A. Furusaki, and A. W. W. Ludwig, Phys. Rev. B **78**, 195125 (2008).
[43] Y. Kim, B. J. Wieder, C. L. Kane, and A. M. Rappe, Phys. Rev. Lett. **115**, 036806 (2015).
[44] R. Yu, H. M. Weng, Z. Fang, X. Dai, and X. Hu, Phys. Rev. Lett. **115**, 036807 (2015).
[45] N. B. Kopnin, T. T. Heikkilä, and G. E. Volovik, Phys. Rev. B **83**, 220503(R) (2011).
[46] G. E. Volovik, Phys. Scr. **T164**, 014014 (2015).
[47] T. T. Heikkilä and G. E. Volovik, arXiv:1504.05824.
[48] M. Z. Hasan and C. L. Kane, Rev. Mod. Phys. **82**, 3045 (2010).
[49] M. M. Nassary, Turk. J. Phys. **33**, 201 (2009).
[50] Z. H. Yu, L. Wang, Q. Y. Hu, J. G. Zhao, S. Yan, K. Yang, S. Sinogeikin, G. D. Gu, and H.-K. Mao, Sci. Rep. **5**, 15939 (2015).
[51] K. Matsubayashi, T. Terai, J. S. Zhou, and Y. Uwatoko, Phys. Rev. B **90**, 125126 (2014).
[52] Y. H. Zhou, X. L. Chen, R. R. Zhang, J. F. Shao, X. F. Wang, C. An, Y. Zhou, C. Y. Park, W. Tong, L. Pi, Z. R. Yang, C. J. Zhang, and Y. H. Zhang, Phys. Rev. B **93**, 144514 (2016).
[53] M. Novak, S. Sasaki, K. Segawa, and Y. Ando, Phys. Rev. B **91**, 041203(R) (2015).
[54] S. Gabáni, E. Bauer, S. Berger, K. Flachbart, Y. Paderno, C. Paul, V. Pavlik, and N. Shitsevalova, Phys. Rev. B **67**, 172406 (2003).
[55] F. F. Tafti, Q. D. Gibson, S. K. Kushwaha, N. Haldolaarachchige, and R. J. Cava, Nat. Phys. **12**, 272 (2015).
[56] C. J. Pickard and R. J. Needs, Phys. Rev. Lett. **97**, 045504 (2006).
[57] C. J. Pickard and R. J. Needs, J. Phys.: Condens. Matter **23**, 053201 (2011).
[58] J. P. Perdew, K. Burke, and M. Ernzerhof, Phys. Rev. Lett. **77**, 3865 (1996).
[59] G. Kresse and J. Furthmüller, Phys. Rev. B **54**, 11169 (1996).
[60] A. A. Mostofi *et al.*, Comput. Phys. Commun. **178**, 685 (2008).
[61] M. P. Lopez Sancho, J. M. Lopez Sancho, J. M. L. Sancho, and J. Rubio, J. Phys. F: Met. Phys. **15**, 851 (1985).
[62] Q. S. Wu, S. N. Zhang, H.-F. Song, M. Troyer, and A. A. Soluyanov, arXiv:1703.07789.
[63] C. Y. Park, D. Popov, D. Ikuta, C. L. Lin, C. Kenney-Benson, E. Rod, A. Bommannavar, and G. Y. Shen, Rev. Sci. Instrum. **86**, 072205 (2015).
[64] C. Prescher and V. B. Prakapenka, High Press. Res. **35**, 223 (2015).
[65] H. K. Mao, J. Xu, and P. M. Bell, J. Geophys. Res. **91**, 4673 (1986).
[66] H. Wiedemeier and F. J. Csillag, Z. Kristallogr. **149**, 17 (1979).
[67] F. Birch, Phys. Rev. **71**, 809 (1947).